EVOLUTIONARY EFFECTS IN THE ORION ASSOCIATION

STEWART SHARPLESS
U.S. Naval Observatory
Received May 16, 1962

ABSTRACT

Photoelectric U, B, V and $H\gamma$ observations are given for stars in the regions of ϵ Orionis and θ^1 Orionis Evolutionary differences between the two regions are discussed, and various age estimates for the subsystems in the Orion association are compared.

I. INTRODUCTION

In Papers I and II (Sharpless 1952, 1954), three-color photometric observations as well as spectral types of a number of members of the Orion association were given, and the Hertzsprung-Russell diagram was constructed. More recently, Blaauw (1958) has brought attention to evolutionary differences within some associations such that the H-R diagram of a dispersed portion of an association may indicate a more advanced evolutionary state than that of a relatively condensed portion. This is reasonable in the light of our current knowledge of expansional motions within associations. An additional problem which was reviewed in Paper I—that of the peculiar reddening in Orion—has been considerably clarified by the recent seven-color photometry of Hallam (1959), who has shown that a strong correlation exists between departures from a linear $1/\lambda$ law of interstellar reddening, on the one hand, and the degree of involvement in emission nebulosity, on the other. The stars immersed in the Orion Nebula were shown by Hallam to exhibit large deviations from the $1/\lambda$ law, while stars outside the nebula have reddening-curves which are more nearly normal.

The purpose of this paper is to examine possible evolutionary differences within the Orion association and to consider whether such differences have a bearing on the problem of photometric distance determinations. Two regions in Orion are compared here. The first is the relatively compact group centered on the Orion Nebula and having a radius of about $1\frac{1}{2}$ degrees. This subsystem will be referred to here as the "Sword." The second region is the relatively dispersed subsystem containing the bright stars δ, ϵ, and ζ Orionis and extending northward approximately to ψ Orionis. An area of 4 square degrees centered on ϵ Orionis has been taken to be representative of this dispersed system and will be referred to here as the "Belt." Three-color photoelectric observations on the U, B, V system have been obtained for all stars in these two regions which have been classified earlier than F0 in the *Henry Draper Extension*. In the Sword region some additional A-type stars from the list of Parenago (1954) were observed. In order to obtain leverage on possible evolutionary effects, an additional datum is desirable which closely correlates with absolute magnitude but is independent of distance and interstellar reddening. Measurements of the absorption of the $H\gamma$ line are known to fulfill these conditions. Accordingly, photoelectric observations of this type have been made for most of the B-type stars in the two regions. In Sections II, III, IV, and V below, these observations are listed and evolutionary differences between the two subsystems are considered.

II. THE OBSERVATIONS

In Tables 1 and 2 the photometric observations are listed. The new U, B, V observation were made with the Ritchey-Chrétien reflector in the same manner as described in Papers I and II, and the probable errors are approximately the same. Some of the data from Papers I and II are repeated here, and some have been improved by additional observations. Column 5 contains the number of individual three-color observa-

TABLE 1

Photometric Observations of Stars in the Region of the Sword of Orion

Star	V	B-V	U-B	N	Hγ(A)	Ey	$(U-B)_o$
-3°1119	10.32	+0.22	+0.13	2	-	+0.06	-
-3°1130	9.48	+ .14	+0.10	1	-	+ .06	-
-3°1140	10.22	+ .26	+0.11	1	14.0	+ .06	-0.08
-3°1143	9.88	+ .17	+0.04	1	12.9	+ .06	-0.09
-3°1146	6.40	- .12	-0.63	1	8.1	+ .06	-0.68
-3°1147	9.29	+ .02	-0.14	1	13.8	+ .06	-0.19
-3°1148	8.36	- .06	-0.37	2	10.7	+ .06	-0.41
-3°1154	9.69	+ .03	-0.09	2	-	+ .06	-
-3°1158	9.94	+ .16	+0.04	1	13.0	+ .06	-0.08
-3°1159	9.80	+ .07	+0.01	1	-	+ .06	-
-3°1171	7.89	- .09	-0.65	1	6.6	+ .06	-0.73
-3°1173	7.70	- .01	-0.11	2	-	+ .06	-
-4°1141	7.53	+ .26	+0.12	2	-	+ .06	-
-4°1142	9.01	+ .30	+0.03	2	-	+ .06	-
-4°1152	7.52	+ .14	+0.10	2	-	+ .06	-
-4°1156	9.71	+ .10	+0.05	1	-	+ .06	-
-4°1158	10.27	+ .21	+0.09	2	-	+ .06	-
-4°1162	8.11	+ .05	-0.49	1	9.1	+ .22	-0.64
-4°1163	8.81	- .05	-0.22	4	13.1	+ .06	-0.23
-4°1164	7.64	+ .02	-0.68	1	7.6	+ .25	-0.86
-4°1165	8.66	+ .34	+0.05	2	-	+ .06	-
-4°1166	8.94	- .01	-0.05	1	-	+ .06	-
-4°1167	6.80	+ .18	+0.11	2	-	+ .06	-
-4°1168	8.09	- .11	-0.51	1	-	+ .06	-
-4°1171	7.40	- .07	-0.43	1	9.6	+ .06	-0.48
-4°1172	7.22	- .08	-0.47	1	-	+ .06	-
-4°1173	6.73	- .10	-0.58	1	9.4	+ .06	-0.64
-4°1175	8.88	+ .07	-0.20	1	-	+ .15	-
-4°1176	7.52	- .11	-0.58	1	-	+ .06	-
-4°1177	9.66	+ .29	+0.03	2	-	+ .06	-
-4°1178	8.83	+ .05	-0.05	1	-	+ .06	-
-4°1179	7.36	- .07	-0.61	1	-	+ .06	-
-4°1180	8.98	.00	-0.21	1	-	+ .06	-
-4°1181	9.55	+ .31	-0.43	3	-	+ .53	-
-4°1183	6.54	- .14	-0.79	1	5.8	+ .06	-0.86
-4°1184	6.22	- .17	-0.69	1	8.3	+ .06	-0.72
-4°1185	4.59	-0.20	-0.94	2	-	+0.06	-

TABLE 1 (Continued)

Star	V	B-V	U-B	N	Hγ(A)	Ey	$(U-B)_o$
-4°1186	6.29	-0.14	-0.71	1	-	+0.06	-
-4°1187	7.34	- .16	-0.74	2	-	+ .06	-
-4°1189	9.97	+ .16	-0.12	3	-	+ .24	-
-4°1190	7.13	- .14	-0.73	1	6.8	+ .06	-0.79
-4°1192	10.96	+ .30	+0.16	2	-	+ .06	-
-4°1196	6.21	- .05	-0.73	2	5.5	+ .18	-0.86
-4°1198	6.85	+ .12	+0.07	2	-	+ .06	-
-4°1199	10.67	+ .35	-0.03	2	-	+ .06	-
-4°1200	9.62	+ .22	0.00	1	13.2	+ .27	-0.17
-4°1201	9.21	+ .01	-0.06	1	-	+ .06	-
-4°1210	7.96	- .09	-0.48	2	9.0	+ .06	-0.52
-4°1211	10.28	+ .15	+0.07	2	-	+ .06	-
-4°1212	9.20	+ .02	-0.07	1	-	+ .06	-
-4°1213	10.10	+ .35	+0.15	2	-	+ .06	-
-4°1214	10.66	+ .36	+0.18	2	-	+ .06	-
-4°1216	9.69	+ .32	+0.14	2	-	+ .06	-
-4°1223	8.53	+ .38	-0.31	1	6.3	+ .57	-0.70
-4°1224	9.69	+ .16	+0.05	1	-	+ .06	-
-5°1247	6.24	- .05	-0.23	7	11.6	+ .06	-0.25
-5°1251	8.72	+ .03	+0.01	2	-	+ .06	-
-5°1252	9.98	+ .35	+0.08	2	-	+ .06	-
-5°1256	9.01	+ .21	+0.09	2	-	+ .06	-
-5°1260	10.27	+ .29	+0.19	2	-	+ .06	-
-5°1269	7.96	- .03	-0.36	2	10.7	+ .06	-0.42
-5°1274	8.64	- .07	-0.39	2	10.5	+ .06	-0.43
-5°1277	9.00	+ .08	+0.05	1	14.1	+ .06	0.00
-5°1281	9.46	+ .75	+0.54	2	-	+ .67	-
-5°1283	10.61	+ .38	+0.02	2	-	+ .06	-
-5°1285	8.74	+ .17	+0.11	2	-	+ .06	-
-5°1287	10.04	+ .30	+0.09	2	-	+ .06	-
-5°1289	8.60	- .04	-0.27	5	11.7	+ .06	-0.30
-5°1300	10.53	+ .24	+0.10	2	-	+ .06	-
-5°1301	9.27	+ .13	+0.08	2	-	+ .06	-
-5°1302	10.25	+ .28	+0.14	2	-	+ .06	-
-5°1304	9.63	+ .05	-0.02	1	-	+ .06	-
-5°1305	7.96	+ .16	+0.03	2	12.6	+ .06	-0.09
-5°1308	9.01	+ .01	-0.28	1	11.0	+ .06	-0.35
-5°1311	7.83	- .10	-0.59	2	8.2	+ .06	-0.65
-5°1312	9.19	.00	-0.20	1	12.9	+ .06	-0.25
-5°1313	8.46	+ .10	-0.62	3	-	+ .33	-
-5°1314	8.48	-0.09	-0.45	2	10.1	+0.06	-0.49

TABLE 1 (Continued)

Star	V	B-V	U-B	N	Hγ(A)	Ey	$(U-B)_o$
-5°1315[a]	6.75	+0.06	-0.92	1	-	+0.38	-
-5°1315[b]	7.96	+ .24	-0.49	1	-	+ .46	-
-5°1315[c]	5.14	+ .06	-0.97	3	-	+ .40	-
-5°1315[d]	6.70	+ .11	-0.64	3	-	+ .35	-
Bond 669	9.62	+ .30	-0.40	2	-	+ .50	-
-5°1316	9.37	+ .04	-0.03	1	-	+ .06	-
-5°1319	5.07	- .05	-0.94	1	-	+ .25	-
-5°1320	6.38	- .05	-0.93	1	-	+ .25	-
-5°1321	9.72	+ .37	+0.01	2	-	+ .06	-
-5°1322	9.79	+ .17	+0.11	2	-	+ .06	-
-5°1323	9.10	- .02	-0.24	1	11.9	+ .06	-0.28
-5°1324	9.83	+ .45	+0.15	2	-	+ .17	-
-5°1325	6.86	+ .29	-0.64	1	5.4	+ .57	-1.05
-5°1326	8.24	+ .05	-0.47	1	8.7	+ .22	-0.62
-5°1327	9.38	+ .02	-0.07	1	-	+ .06	-
-5°1328	9.89	+ .09	+0.02	1	-	+ .06	-
-5°1330	7.08	- .06	-0.57	2	7.1	+ .06	-0.66
-5°1331	8.99	- .04	-0.12	1	12.8	+ .06	-0.12
-5°1334	6.57	- .19	-0.82	2	6.9	+ .06	-0.85
-5°1335	9.17	- .03	-0.14	1	13.6	+ .06	-0.15
-5°1336	8.62	+ .30	+0.09	2	-	+ .06	-
-5°1337	10.69	+ .28	+0.10	2	-	+ .06	-
-5°1338	9.17	+ .28	+0.09	2	-	+ .06	-
-5°1342	7.19	- .17	-0.77	1	6.2	+ .06	-0.81
-5°1346	9.88	+ .16	+0.11	1	-	+ .06	-
-5°1347	7.64	+ .33	+0.17	2	-	+ .06	-
-5°1348	9.56	+ .16	+0.07	2	-	+ .06	-
-5°1351	7.61	- .12	-0.56	4	8.3	+ .06	-0.60
-5°1352	10.42	+ .66	+0.44	2	-	+ .50	-
-5°1365	10.12	+ .26	+0.11	2	-	+ .06	-
-5°1369	9.45	+ .34	+0.14	2	-	+ .06	-
-5°1370	9.10	+ .04	-0.06	1	-	+ .06	-
-5°1377	9.77	+ .46	+0.34	2	-	+ .36	-
-6°1185	9.64	+ .32	+0.06	2	-	+ .06	-
-6°1204	8.09	+ .12	-0.02	1	-	+ .06	-
-6°1207	6.23	- .15	-0.77	1	7.6	+ .06	-0.83
-6°1209	7.69	- .08	-0.45	1	10.0	+ .06	-0.49
-6°1212	8.28	- .09	-0.41	1	9.9	+ .06	-0.44
-6°1216	9.23	- .04	-0.16	1	14.1	+ .06	-0.17
-6°1217	8.69	+ .17	+0.07	1	-	+ .06	-
-6°1223	9.81	+ .13	+0.07	2	-	+ .06	-
-6°1226	9.50	+0.01	-0.11	1	-	+0.06	-

TABLE 1 (Continued)

Star	V	B-V	U-B	N	Hγ(A)	Ey	$(U-B)_o$
-6°1227	8.56	+0.07	-0.23	2	-	+0.17	-
-6°1233	5.67	- .22	-0.93	1	4.7	+ .06	-0.96
-6°1234	4.77	- .25	-1.04	2	5.8	+ .06	-1.06
-6°1237	7.49	- .13	-0.67	2	8.2	+ .06	-0.72
-6°1238	8.89	- .06	-0.27	1	12.5	+ .06	-0.29
-6°1240	7.17	- .12	-0.63	2	8.2	+ .06	-0.68
-6°1241[e]	2.75	- .25	-1.07	2	3.2	+ .06	-1.10
-6°1242	9.40	+ .10	+0.05	2	-	+ .06	-
-6°1244	9.82	+ .14	+0.08	2	-	+ .06	-
-6°1247	8.32	- .02	-0.44	2	9.7	+ .06	-0.53
-6°1254	8.10	- .07	-0.41	1	10.7	+ .06	-0.53
-6°1255	5.71	- .23	-0.93	1	5.4	+ .06	-0.95
-6°1257	9.60	+ .14	+0.05	2	-	+ .06	-
-6°1262	6.02	- .20	-0.96	1	5.9	+ .06	-1.01
-6°1263	10.53	+ .36	+0.04	2	-	+ .06	-
-6°1264	8.85	+ .12	+0.01	1	13.5	+ .06	-0.08
-6°1265	9.50	+ .31	+0.05	2	-	+ .06	-
-6°1267	8.30	- .09	-0.41	1	9.9	+ .06	-0.44
-6°1268	9.48	+ .17	-0.09	1	12.2	+ .24	-0.25
-6°1270	9.82	+ .11	+0.01	1	-	+ .06	-
-6°1271	8.82	+ .15	-0.23	1	9.8	+ .26	-0.40
-6°1273	10.33	+ .31	-0.05	3	11.1	+ .40	-0.31
-6°1274	8.22	+ .06	-0.27	1	10.4	+ .16	-0.38
-6°1275	5.96	- .23	-0.92	7	5.5	+ .06	-0.94
-6°1277	8.67	+ .15	+0.09	1	-	+ .06	-
-6°1278	9.33	.00	-0.10	1	13.5	+ .06	-0.12
-6°1281	9.19	- .02	-0.09	1	13.0	+ .06	-0.10
-6°1286	9.21	+ .05	-0.05	1	12.9	+ .06	-0.10
-6°1291	9.56	+ .24	+0.12	2	-	+ .06	-
-6°1297	9.22	+ .06	+0.01	1	-	+ .06	-
-6°1300	10.25	+ .31	+0.05	2	-	+ .06	-
-7°1081	9.68	+ .12	+0.04	2	-	+ .06	-
-7°1083	9.04	- .02	-0.14	1	11.4	+ .06	-0.16
-7°1092	6.71	- .13	-0.57	1	7.7	+ .06	-0.60
-7°1096	9.25	+ .15	+0.05	2	-	+ .06	-
-7°1099	6.33	- .17	-0.86	1	5.5	+ .06	-0.92
-7°1100	10.86	+ .26	+0.05	1	-	+ .06	-
-7°1103	7.81	- .11	-0.54	1	8.4	+ .06	-0.58
-7°1105[f]	9.50	+ .03	-0.11	1	-	+ .06	-
-7°1106	4.61	- .25	-1.08	29	3.4	+ .06	-1.11
-7°1108	9.95	+ .32	+0.06	2	-	+ .06	-
-7°1115	8.67	+0.06	-0.04	1	13.6	+0.06	-0.10

TABLE 1 (Continued)

Star	V	B-V	U-B	N	Hγ(A)	Ey	$(U-B)_o$
-7°1122	9.30	-0.02	-0.16	1	-	+0.06	-
-7°1131	7.40	- .08	-0.40	1	9.7	+ .06	-0.43
-7°1137	10.24	+ .17	+0.14	2	-	+ .06	-
-7°1139	9.72	+ .23	+0.11	2	-	+ .06	-
-7°1151	7.67	- .12	-0.70	2	6.7	+ .06	-0.77
P 106	11.60	+ .44	+0.31	2	-	+ .31	-
P 162	10.83	+ .36	+0.10	2	-	+ .06	-
P 571	10.82	+ .52	+0.35	2	-	+ .38	-
P 612	10.80	+ .41	-0.01	2	-	+ .06	-
P 880	10.41	+ .38	+0.09	2	-	+ .06	-
P 1212	11.41	+ .73	+0.41	2	-	+ .50	-
P 1355	12.15	+ .66	+0.33	2	-	+ .41	-
P 1539	10.74	+ .73	+0.29	2	-	+ .81 :	-
P 1683	10.91	+ .46	+0.36	2	-	+ .42 :	-
P 1712	10.49	+ .56	+0.27	2	-	+ .60	-
P 2632	11.84	+ .79	+0.56	2	-	+ .73 :	-
P 2652	11.43	+ .92	+0.33	2	-	+1.02 :	-
P 2840	11.09	+ .43	+0.06	2	-	+ .06	-
P 2904	10.44	+ .71	+0.50	2	-	+ .64 :	-
P 2942	12.23	+0.73	+0.41	2	-	+0.76 :	-

TABLE 2

Photometric Observations of Stars in the Region of the Belt of Orion

Star	V	B-V	U-B	N	Hγ(A)	Ey	$(U-B)_o$
-0°989	8.94	-0.03	-0.27	2	-	+0.07	-
-0°991	9.09	+ .24	+0.12	2	-	+ .07	-
-0°992	8.34	- .04	-0.19	2	-	+ .07	-
-0°993	8.81	+ .08	+0.06	2	-	+ .07	-
-0°996	7.63	- .10	-0.42	2	9.6	+ .07	-0.44
-0°997	9.31	.00	-0.08	2	-	+ .07	-
-0°999	8.65	+ .04	-0.13	2	12.9	+ .07	-0.19
-0°1002	8.62	+ .03	-0.35	2	10.9	+ .15	-0.46
-0°1003	9.81	+ .09	+0.01	2	-	+ .07	-
-0°1004	9.68	+ .06	+0.04	2	-	+ .07	-
-0°1005	7.04	- .07	-0.43	2	8.1	+ .07	-0.48
-0°1006	8.01	- .01	-0.34	2	10.1	+ .07	-0.41
-0°1007	7.51	- .12	-0.55	2	8.4	+ .07	-0.59
-0°1008	9.44	+ .10	-0.04	2	13.7	+ .07	-0.13
-0°1009	6.92	- .09	-0.66	2	7.7	+ .07	-0.74
-0°1010	10.30	+ .35	+0.06	2	-	+ .07	-
-0°1012	10.25	+ .19	+0.12	2	-	+ .07	-
-0°1014	10.36	+ .18	+0.10	2	-	+ .07	-
-0°1015	9.83	+ .19	+0.06	2	-	+ .07	-
-0°1016	8.81	+ .04	0.00	2	-	+ .07	-
-0°1017	8.01	- .08	-0.49	2	8.4	+ .07	-0.54
-0°1018	8.55	+ .09	-0.39	2	8.3	+ .24	-0.55
-0°1020	10.67	+ .26	+0.15	2	-	+ .07	-
-0°1022	9.41	+ .06	+0.03	2	-	+ .07	-
-0°1023	8.17	- .10	-0.44	2	8.9	+ .07	-0.47
-0°1024	8.93	+ .06	-0.02	2	-	+ .07	-
-0°1025	8.69	- .03	-0.08	2	-	+ .07	-
-0°1027	8.97	+ .12	+0.04	2	-	+ .07	-
-0°1028	8.35	- .08	-0.33	2	-	+ .07	-
-0°1029	9.11	- .02	-0.11	2	-	+ .07	-
-0°1031	7.59	- .12	-0.60	2	9.0	+ .07	-0.65
-0°1033	8.69	+ .10	-0.02	2	-	+ .07	-
-0°1034	7.45	- .04	-0.42	2	9.5	+ .07	-0.49
-0°1035(E)	8.83	+ .05	-0.13	1	-	+ .07	-
-0°1035(W)	8.66	+ .14	-0.05	1	-	+ .07	-
-0°1036	8.62	- .03	-0.30	2	9.8	+ .07	-0.35
-0°1038	10.54	+ .25	+0.11	2	-	+ .07	-
-0°1039	10.61	+ .34	+0.14	2	-	+ .07	-
-0°1040	10.19	+0.17	+0.10	2	-	+0.07	-

TABLE 2 (Continued)

Star	V	B-V	U-B	N	Hγ(A)	Ey	$(U-B)_o$
-0°1046	10.42	+0.40	+0.32	2	-	+0.34	-
-0°1047	10.63	+ .21	+0.06	2	-	+ .07	-
-0°1050	10.15	+ .57	+0.11	2	-	+ .66	-
-1°934	10.22	+ .17	+0.07	2	-	+ .07	-
-1°935	5.31	- .19	-0.95	2	4.7	+ .07	-1.01
-1°939	6.51	- .10	-0.64	1	8.0	+ .07	-0.71
-1°941	9.11	+ .01	-0.20	2	11.4	+ .07	-0.26
-1°942	8.66	.00	-0.12	2	13.1	+ .07	-0.15
-1°943	5.31	- .17	-0.92	2	5.2	+ .07	-0.99
-1°944	10.20	+ .11	+0.09	2	-	+ .07	-
-1°945	10.04	+ .32	+ .11	2	-	+ .07	-
-1°947	10.44	+ .16	+0.13	2	-	+ .07	-
-1°948	8.52	+ .03	-0.40	2	9.1	+ .17	-0.52
-1°949	6.24	- .19	-0.81	2	5.1	+ .07	-0.84
-1°952	8.29	+ .28	+0.18	2	-	+ .21	-
-1°955	9.47	+ .13	+0.01	2	-	+ .07	-
-1°957	9.57	+ .04	-0.03	2	-	+ .07	-
-1°963	9.53	+ .15	-0.02	2	-	+ .07	-
-1°964	9.37	+ .03	-0.04	2	-	+ .07	-
-1°965	8.10	- .09	-0.41	2	9.6	+ .07	-0.44
-1°966	9.01	- .02	-0.13	2	-	+ .07	-
-1°968	8.65	+ .05	-0.13	2	13.5	+ .07	-0.20
-1°969[g]	1.66	- .18	-1.03	1	2.7	+ .07	-1.11
-1°970	10.04	+ .20	+0.08	2	12.9	+ .07	-0.06
-1°971	8.02	- .09	-0.50	2	8.6	+ .07	-0.55
-1°973	8.30	+ .12	+0.04	2	-	+ .07	-
-1°974	8.13	- .01	-0.23	4	10.8	+ .07	-0.28
-1°975	9.80	+ .34	+0.19	2	-	+ .07	-
-1°976	10.18	+ .15	+0.09	2	-	+ .07	-
-1°977	9.79	+ .06	+0.02	2	-	+ .07	-
-1°978	9.22	+ .05	-0.18	2	11.6	+ .07	-0.26
-1°979	7.92	- .10	-0.54	2	8.4	+ .07	-0.59
-1°980	9.02	+ .04	-0.04	2	-	+ .07	-
-1°981	10.69	+ .47	+0.25	2	-	+ .07	-
-1°982	7.08	- .08	-0.55	2	7.8	+ .07	-0.62
-1°983	9.07	+ .01	-0.07	2	-	+ .07	-
-1°984	8.75	- .03	-0.17	2	-	+ .07	-
-1°985	8.38	- .07	-0.37	2	-	+ .07	-
-1°986	9.87	+ .20	+0.10	2	-	+ .07	-
-1°987	6.83	- .15	-0.75	2	6.5	+ .07	-0.80
-1°994	9.26	+0.05	-0.04	2	14.0	+0.07	-0.09

TABLE 2 (Continued)

Star	V	B-V	U-B	N	Hγ(A)	Ey	$(U-B)_o$
-1°995	9.29	+0.03	-0.08	2	-	+0.07	-
-1°998	8.56	+ .13	+0.13	2	-	+ .07	-
-1°1001	7.68	- .08	-0.58	2	6.4	+ .07	-0.65
-1°1004	4.91	- .22	-0.85	2	5.5	+ .07	-0.87
-1°1005	6.97	- .14	-0.86	2	4.5	+ .07	-0.94
-1°1006	8.80	+ .10	+0.09	2	-	+ .07	-
-1°1009	8.79	- .01	-0.12	2	-	+ .07	-
-2°1287	9.33	+ .28	+0.16	2	-	+ .07	-
-2°1294	7.08	+ .18	+0.12	2	13.7	+ .07	0.00
-2°1303	9.01	+ .04	-0.09	2	-	+ .07	-
-2°1333[h]	7.56	- .06	-0.38	3	10.6	+ .07	-0.42
-2°1338[h]	1.72	- .21	-1.05	2	2.6	+ .07	-1.11
290570	11.13	+ .32	+0.19	2	-	+ .07	-
290600	10.64	+ .38	+0.14	2	-	+ .07	-
290605	10.13	+ .17	+0.09	2	-	+ .07	-
290656	10.60 :	+ .25	+0.09	2	-	+ .07	-
290659	11.02	+ .38	+0.17	2	-	+ .07	-
290661	10.74	+ .34	+0.07	2	-	+ .07	-
290678	10.69	+ .21	+0.05	2	-	+ .07	-
290686	11.06	+ .34	+0.15	2	-	+ .07	-
290691	10.30	+ .20	+0.10	2	-	+ .07	-
290695	10.03	+ .48	+0.04	2	-	+ .58	-
290732	10.10	+ .13	+0.07	2	-	+ .07	-
290733	10.29	+ .43	+0.01	2	-	+ .52	-
290739	11.44	+ .31	+0.17	2	-	+ .07	-
290740	11.66	+ .23	+0.18	2	-	+ .07	-
290744	11.16	+ .33	+0.13	2	-	+ .07	-
290745	10.52	+ .25	+0.11	2	-	+ .07	-
290748	10.20	+ .17	+0.11	2	-	+ .07	-
290758	10.95	+ .34	+0.22	2	-	+ .07	-
290761	11.38	+ .50	+0.32	2	-	+ .36 :	-
290764	9.88	+ .32	+0.09	2	-	+ .07	-
290766	10.64	+ .30	+0.20	2	-	+ .07	-
290768	10.41	+ .56	+0.35	2	-	+ .41	-
290813	11.00	+0.51	+0.20	2	12.3	+0.56	-0.17

NOTES TO TABLES 1 AND 2

[a] θ^1(A) Orionis
[b] θ^1(B) Orionis
[c] θ^1(C) Orionis
[d] θ^1(D) Orionis
[e] ι Orionis
[f] υ Orionis
[g] ϵ Orionis
[h] ζ Orionis

tions. The photoelectric Hγ observations were made through interference filters, one having a band width of approximately 30 A and a comparison filter having the same effective wavelength and a band width of 150 A. The comparison filter was combined with a neutral filter, in order approximately to equalize the two deflections. A number of standard stars from Petrie's (1953) list were observed, in order to effect a conversion of the photoelectric observations to units of equivalent angstroms. The Hγ observations are listed in column 6. Generally, each star was observed once. The internal probable error of an Hγ observation is estimated to be approximately ±0.4 A.

Column 7 contains the estimated color excess. From an inspection of the two-color diagram it was found that a mean color excess can be applied to the majority of stars in the two regions: $\bar{E}_y = 0.06$ for the Sword region, and $\bar{E}_y = 0.07$ for the Belt. In the case of those stars whose colors indicate an appreciably greater reddening, individual estimates were made by means of the Q-method or, for stars of types later than A0, its graphical equivalent. The assignment of a mean color excess to the majority of stars in the two regions may not result in the most accurate reddening estimate for a particular star, but this method has the advantage of preserving as well as possible the true distribution of stars along the main sequence. A blanket application of the Q-method or its graphical equivalent can bias the observed numbers of late B- and early A-type stars.

The intrinsic ultraviolet colors are given in column 8. These were computed on the basis of the precepts given by Johnson (1958*a*).

III. EVOLUTIONARY EFFECTS

In Figures 1 and 2 the Hγ measure is plotted against $(U - B)_0$ for the B-type stars in the two regions. A straight-line fit is adequate in both cases. Least-squares solutions yield

$$\text{Sword: } \mathrm{H}\gamma = 14.3 + 9.3\,(U - B)_0\,,$$

$$\text{Belt: } \mathrm{H}\gamma = 14.3 + 10.0\,(U - B)_0\,.$$

The line representing the Belt stars thus lies significantly higher than that corresponding to the Sword for values of $(U - B)_0 < 0.00$. A systematic difference in the Hγ measures for the two subsystems apparently exists in the sense that the stars in the Belt region have, on the average, weaker hydrogen lines and are therefore intrinsically more luminous. This effect has already been noted qualitatively by Morgan (1956, 1958). The average difference in luminosity between the two groups will be discussed below.

The color-magnitude diagrams for the two regions, corrected for interstellar absorption, are shown in Figures 3 and 4. In accordance with the results of Hallam (1959), a normal ratio of total to selective absorption has been applied except for the five stars which are immersed in the Nebula, in which case double the normal ratio has been assumed. The solid lines in Figures 3 and 4 have been drawn in each case to represent the lower envelopes of the plotted points, some allowance having been made for scatter due to observational errors. There are several reasons for adopting curves of this type: (1) the lower envelope is sharply defined and is not influenced by the effects of duplicity or the presence of foreground stars, and (2) it is in keeping with the current concept of an "unevolved" main sequence, in that the latter presumably represents the lower envelope of the evolutionary tracks of stars in the color-magnitude diagram. A comparison of the two envelopes, shown in Figure 5, indicates that they do not coincide but differ by −0.1 to +0.4 mag in the range of $(B - V)_0$ between 0.00 and −0.25 mag. That this discrepancy is intrinsic rather than due to differences in distance is borne out by the Hγ measures. The comparison is given in detail in Table 3*A*, where, for different values of $(B - V)_0$, the average difference in absolute magnitude, ΔM_γ, as derived from the Hγ measures, is compared with the corresponding difference in apparent magnitude,

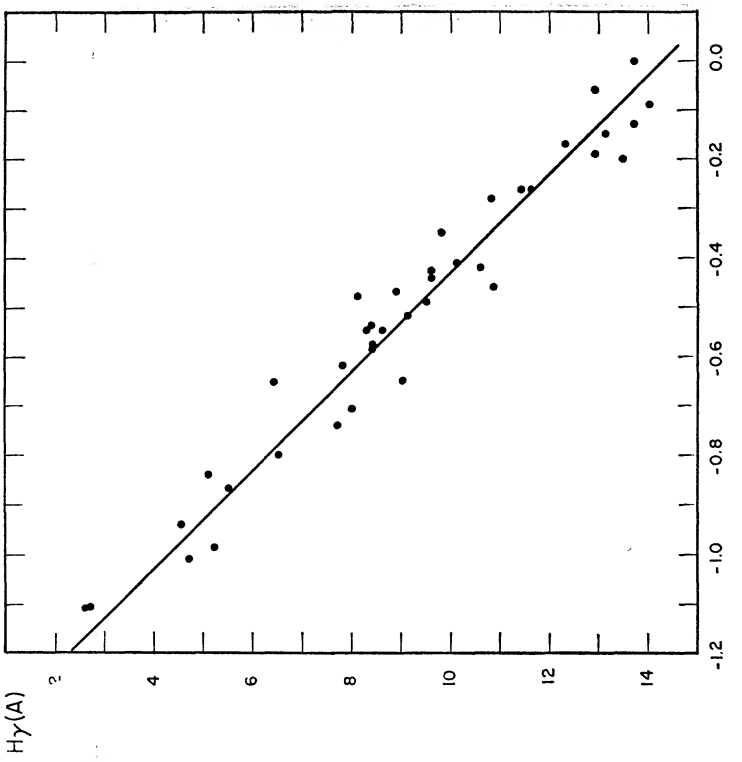

FIG. 2.—The Hγ measure, in equivalent angstroms, plotted against the intrinsic ultraviolet color for stars in the Belt region of Orion.

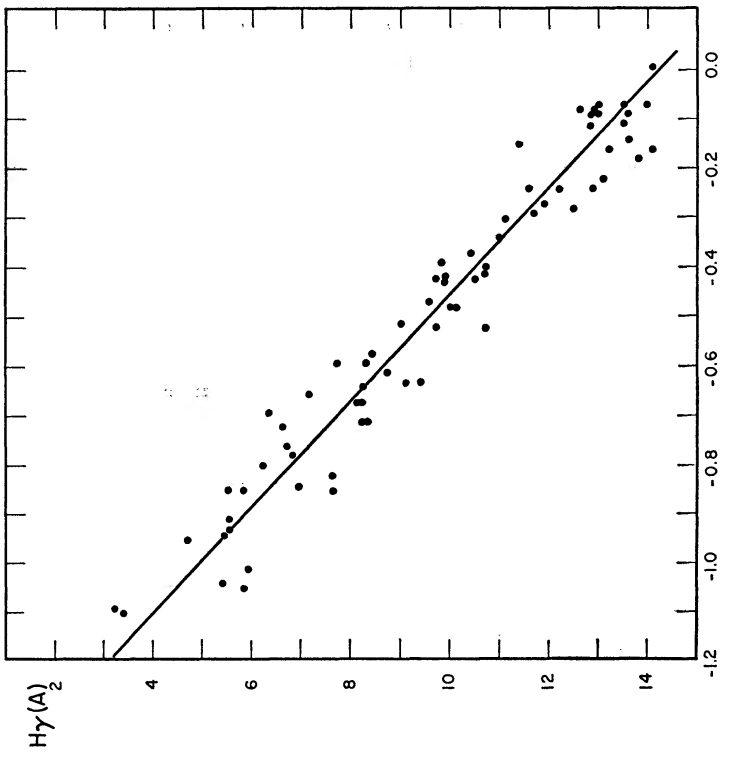

FIG. 1.—The Hγ measure, in equivalent angstroms, plotted against the intrinsic ultraviolet color for stars in the Sword region of Orion.

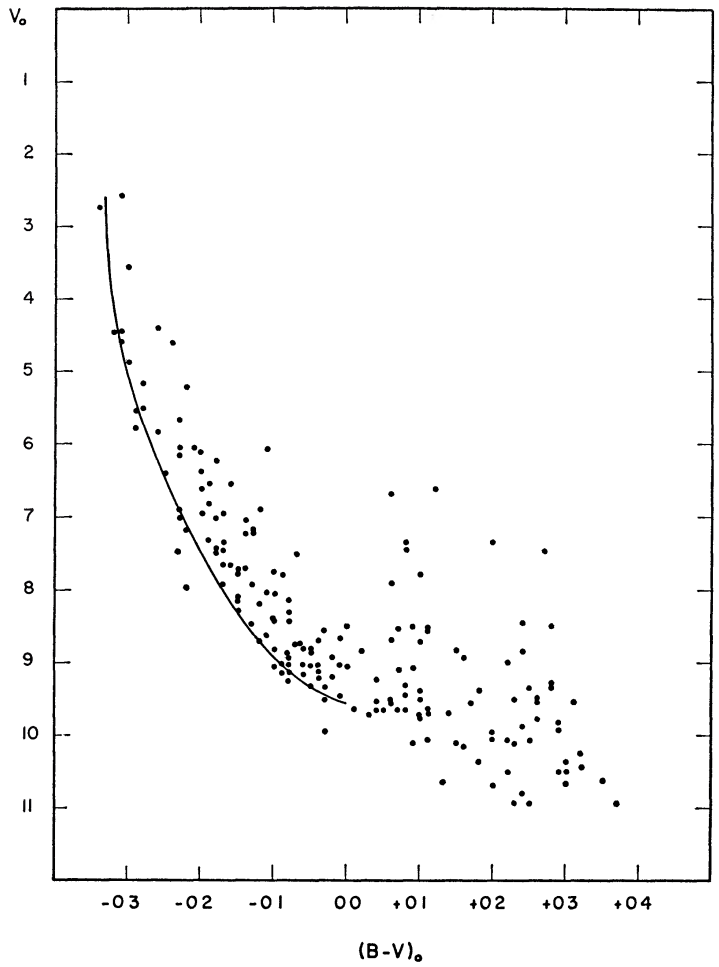

FIG. 3.—The color-magnitude diagram, corrected for interstellar absorption, for stars in the Sword region of Orion.

TABLE 3A

COMPARISON OF MAIN SEQUENCES OF THE SWORD AND BELT REGIONS

$(B-V)_0$	$\Delta H\gamma$ (A)	ΔM_γ (mag)	ΔV_0 (mag)
0 00	0.00	0 00	−0 1
− .05	.10	.10	+ 1
− .10.....	.25	.15	+ .2
− .15	.37	.15	+ 2
− .20... . .	52	.30	+ 3
−0.25	0.64	0 65	+0.4

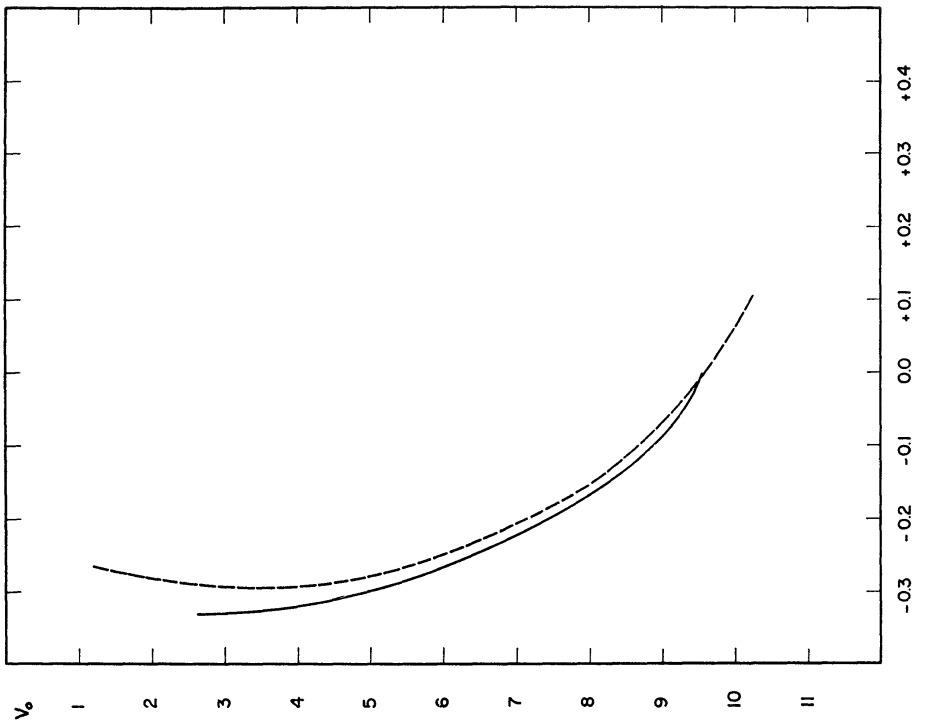

FIG. 5.—Lower envelopes of the main sequences of the Sword region (*solid*) and Belt region (*dashed*) of Orion.

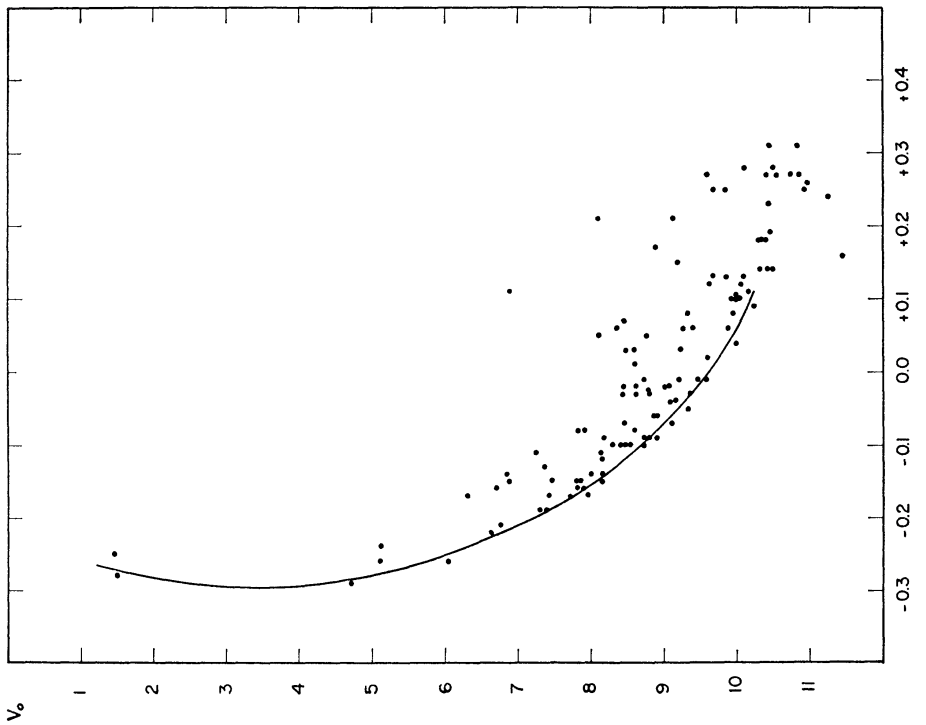

FIG. 4.—The color-magnitude diagram, corrected for interstellar absorption, for stars in the Belt region of Orion.

ΔV_0, for the two main sequences as derived from the color-magnitude diagrams. The values of ΔM_γ were obtained differentially from Johnson's (1958*b*) calibration. The two independent sets of data, ΔM_γ and ΔV_0, both indicate a similar relative displacement of the two main sequences. It is concluded that this displacement is intrinsic rather than due to a difference in the distances of the two subsystems.

The position and extent of the lower end of the two main sequences are of interest, insofar as some of the fainter members may still be in a stage of gravitational contraction. Counts of stars belonging to the various spectral subclasses were made on the basis of the data contained in the *Henry Draper Extension*. These results are shown in Figure 6.

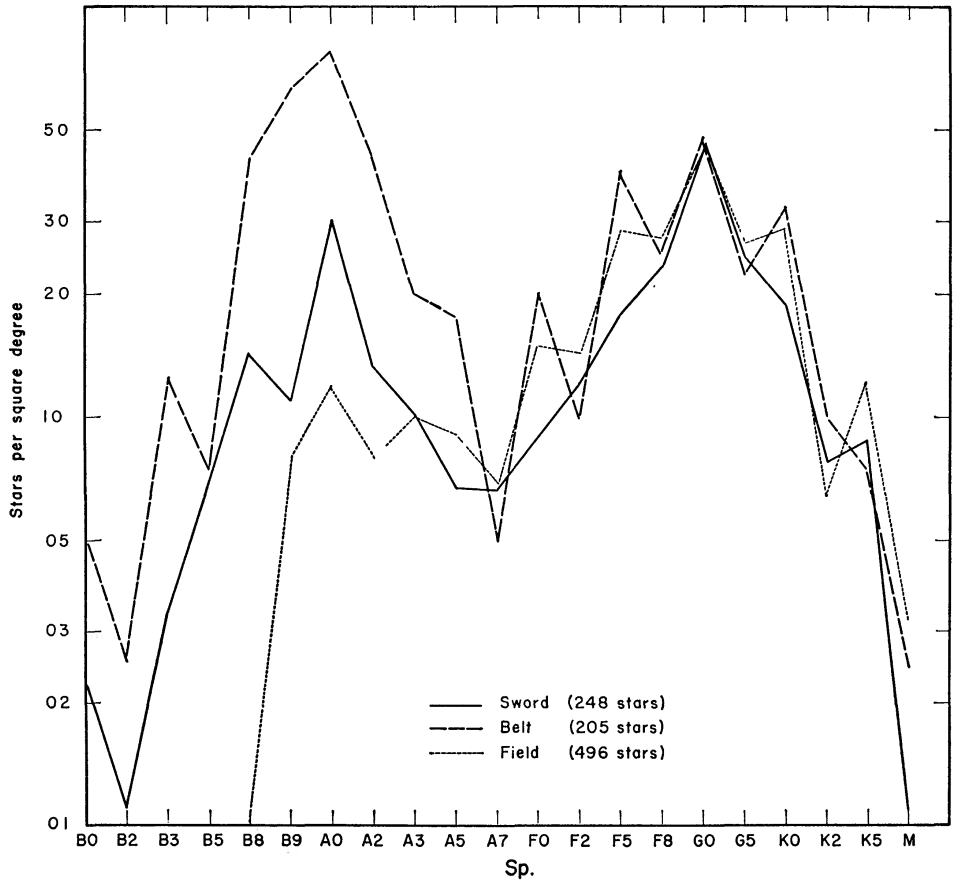

FIG. 6.—Counts of stars of various spectral types in the *Henry Draper Extension* for the Sword and Belt regions of Orion, as well as comparison regions outside the association.

The line marked "field" represents counts in three sample areas which are outside the association but which share the same mean galactic co-ordinates as the two subsystems. The stars from whose data the color-magnitude diagrams in Figures 3 and 4 were constructed were also selected, for the most part, to the limit of the *Henry Draper Extension*. Therefore, the counts of Figure 6 and the color-magnitude diagrams may properly be regarded as referring to the same stars. Figure 6 indicates that there is no noticeable excess of members in the Belt region later than A5 and no excess in the Sword later than A2. The color-magnitude diagrams indicate the existence of a main sequence to about $(B - V)_0 = +0.13$ for the Belt and to about $(B - V)_0 = +0.10$ for the Sword. The color-magnitude diagrams and the counts are therefore in agreement in indicating the

lower extent of a noticeably populated main sequence for the two regions. The stars later than about $(B - V)_0 = +0.13$ cannot all be considered members of the association, even though they occupy the region of the color-magnitude diagram customarily associated with stars which are still in a state of gravitational contraction. In the range of $(B - V)_0$ between -0.05 and $+0.10$, the main sequence of the Sword stars shows a definite turn-up, thus indicating the existence of contracting stars in this range and confirming Strand's (1958) conclusion that the departure from the unevolved main sequence has already taken place at A0 for the stars in the vicinity of the Orion Nebula.

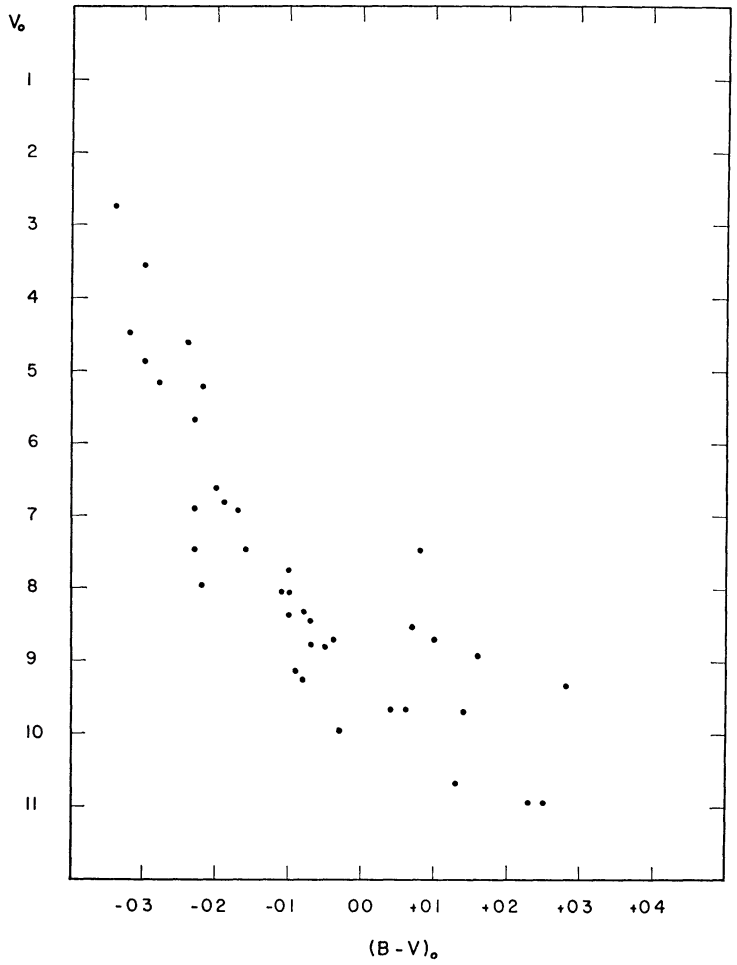

FIG. 7.—The color-magnitude diagram for those stars in the Sword region of Orion which show a high degree of reddening.

The counts discussed here do not show that there are no contracting stars in the two subsystems redder than $(B - V)_0 = +0.13$. On the other hand, they do indicate that such stars, if they exist, are not very numerous compared with the contribution due to the field; consequently, the presence of contracting stars must be established by some criterion other than their position in the color-magnitude diagram. Radial-velocity or proper-motion data are valuable for this purpose when available. In the case of the Orion stars, large color excess is a sufficient, though not necessary, condition of membership, since the foreground stars are virtually unreddened. Figure 7 contains the color-magnitude diagram for only those stars in the Sword region with high color excesses.

Evidently some of the stars later than A0 lie approximately on the unevolved main sequence, while four or five lie above it by a significant amount and may be stars which are still contracting toward the main sequence.

IV. THE DISTANCE AND AGES OF THE SUBSYSTEMS IN ORION

It is possible to obtain an improved distance modulus of the Orion association which takes into account evolutionary effects. This can be obtained most directly through a comparison with the Scorpio-Centaurus association, for which fundamentally determined absolute magnitudes are available (Bertiau 1958). Johnson (1959) has published Hγ observations for a number of the members. The plot of Hγ absorption versus $(U - B)_0$ for the Scorpio-Centaurus stars indicates an evolutionary state intermediate between those of the Sword and Belt regions of Orion, and, allowance having been made for this, a comparison of the respective color-magnitude diagrams yields a distance modulus of 8.2 mag. for the Orion association. This can be compared with the value of 8.3 mag. obtained by Blaauw (1958) through a comparison of the H-R diagram of the Belt region

TABLE 3B

MAIN SEQUENCES OF FIGURES 3 AND 4

M_v	$(B-V)_0$	
	Sword	Belt
+1.0	−0.04	−0 02
0 0	− .14	− .13
−1 0	− .20	− .19
−2 0	− 25	− 23
−3 0	− 29	− .27
−4 0	− 31	− 29
−5 0	−0 33	− 30
−6 0.	.	− 29
−7 0	. .	−0 27

of Orion with that of the upper (more dispersed) Scorpio section of the Scorpio-Centaurus association. An astrometric distance modulus, independent of evolutionary effects, of 8.6 mag. has been obtained by Strand (1958) through a comparison of the velocity dispersion along the line of sight with the proper-motion dispersion in the tangential plane for stars in the region of the Orion Nebula. A straight mean of these three determinations is adopted here:

$$M - m_0 = 8.4 \pm 0.2 \text{ mag.}$$

On the basis of this distance modulus and the main sequences of Figures 3 and 4, the values of $(B - V)_0$ corresponding to various absolute magnitudes are listed in Table 3*B*.

The ages of groups of young stars can be estimated in several ways: (1) kinematic ages depending on the relative motions of stars which are presumed to have had a common origin and (2) ages depending on certain features of the color-magnitude diagram as interpreted by theories of stellar evolution. A number of age estimates for various subsystems in the Orion association are summarized in Table 4. An intercomparison of the ages given there indicates at least three different epochs of star formation in Orion. The youngest stars are the components of the Trapezium, whose relative motions indicate an age of 10^4 years or less. The relative motions of the members of the cluster surrounding the Orion Nebula indicate an age that is in agreement with that determined on the basis of the color-magnitude diagram, i.e., about $3–5 \times 10^5$ years. The color-magnitude

diagram for the Belt region indicates an age about an order of magnitude greater. Apparently, the "runaway" stars are more logically to be associated with the Belt subsystem than with the subsystem centered on the Orion Nebula, since their ages agree much more closely with that of the former. The large variety of ages given in Table 4 suggests that star formation in the Orion association has been a sporadic, or discontinuous, phenomenon.

V. CONCLUSIONS

It has been shown that (1) star formation in the Orion association has apparently taken place at various epochs, and differences in the ages of the subsystems are reflected in differences between their respective color-magnitude diagrams. A single standard main sequence cannot apply to both subsystems studied here. The determination of the

TABLE 4

AGE DETERMINATIONS FOR STARS IN THE ORION AGGREGATE

Method	Age (years)	Reference*
Relative motions of members of the Trapezium	$<10^4$	1
Relative motions in the Orion Nebula Cluster	3×10^5	2
Runaway stars (AE Aur, μ Col, 53 Ari).	2 2–4 9×10^6	3
Color-magnitude diagram of the Belt subsystem	$\sim5\times10^6$	4
Color-magnitude diagram of the Sword subsystem	$\sim5\times10^5$	4

*The references are as follows:
1 Parenago (1953)
2 Strand (1958)
3 Blaauw (1961).
4 Estimated by the author on the basis of the computations of von Hoerner (1957)

distance of a group of young stars by fitting the observed color-magnitude diagram to a "standard" main sequence is apparently a method which should be applied with circumspection. An additional datum, such as Hγ intensity, can lend considerably more weight to such determinations by allowing evolutionary differences to be taken into account. (2) In the case under discussion, three colors alone are not sufficient to identify the faint members, owing to the large admixture of field stars.

REFERENCES

Bertiau, F. C. 1958, *Ap. J.*, **128**, 533.
Blaauw, A. 1958, *A.J.*, **63**, 186.
———. 1961, *B.A.N.*, **15**, 265.
Hallam, K. 1959, Doctoral thesis, University of Wisconsin
Hoerner, S. van. 1957, *Zs. f. Ap*, **42**, 273.
Johnson, H. L. 1958*a*, *Lowell Obs. Bull*, **4**, 37.
———. 1958*b*, *ibid.*, p. 47.
———. 1959, *ibid.*, p. 87.
Morgan, W. W. 1956, *A.J.*, **61**, 358
———. 1958, *Trans. I.A.U.*, **10**, 576.
Parenago, P. P. 1953, *Russ. A.J.*, **30**, 249
———. 1954, *Trudy Sternberg Astr. Inst.*, Vol. **25**.
Petrie, R M. 1953, *Dom. Ap. Obs*, **9**, 251.
Sharpless, S. 1952, *Ap. J.*, **116**, 251.
——— 1954, *ibid.*, **119**, 200.
Strand, K. Aa. 1958, *Ap. J.*, **128**, 14.